Effect of Thinned-Skull Cranial Window on Monitoring Cerebral Blood Flow Using Laser Speckle Contrast Imaging

Nadezhda Golubova, Ivan Ryzhkov, Konstantin Lapin, Evgeniya Seryogina, Andrey Dunaev, Viktor Dremin, and Elena Potapova

***Abstract*—Studies on laboratory animals are a crucial step in a wide range of fundamental and applied scientific investigations. In addition to ensuring that research methods are chosen correctly, it is also necessary to use them properly in order to obtain the maximum amount of reliable information. In this study, we analyze and compare laser speckle contrast imaging (LSCI) data obtained simultaneously from the intact skull area and from the thinned skull area of the young laboratory rat (1.5-months-old), while additionally introducing a physiological challenge in the form of blood loss. We describe the experimental setup and materials used and also outline the signal processing approach. Finally, we present the results obtained and provide a discussion comparing our findings with studies conducted by other researchers, as well as addressing both the highlights and limitations of the study. In summary, the investigations conducted indicate that a cranial preparation is needed to record reliable LSCI data for cerebral perfusion, and it is also found that moderate blood loss does not reduce cerebral blood flow to the level of its autoregulation impairment.**

***Index Terms*—Laser speckle contrast imaging (LSCI), cerebral blood flow dynamics, thinned-skull cranial window, blood loss.**

Received 27 April 2024; revised 14 November 2024; accepted 22 January 2025. Date of publication 27 January 2025; date of current version 5 February 2025. This work was supported by Russian Science Foundation under Project 24-25-00310. *(Corresponding author: Viktor Dremin.)*

This work involved human subjects or animals in its research. Approval of all ethical and experimental procedures and protocols was granted by the Ethics Committee of Orel State University under Application No. 27 dated 17/05/2023, and performed in line with the European Union guidelines for the care of laboratory animals (Directive 2010/63/EU).

Nadezhda Golubova is with the R&D Center of Biomedical Photonics, Orel State University, 302026 Orel, Russia, and also with the Federal Research and Clinical Center of Intensive Care Medicine and Rehabilitology, 141534 Moscow, Russia (e-mail: nadin.golubova@inbox.ru).

Ivan Ryzhkov and Konstantin Lapin are with the Federal Research and Clinical Center of Intensive Care Medicine and Rehabilitology, 141534 Moscow, Russia (e-mail: iryzhkov@fnkcrr.ru; k.n.lapin@gmail.com).

Evgeniya Seryogina, Andrey Dunaev, and Elena Potapova are with the R&D Center of Biomedical Photonics, Orel State University, 302026 Orel, Russia (e-mail: e.s.seryogina@gmail.com; dunaev@bmecenter.ru; e.potapova@oreluniver.ru).

Viktor Dremin is with the R&D Center of Biomedical Photonics, Orel State University, 302026 Orel, Russia, and also with the College of Engineering and Physical Sciences, Aston University, B4 7ET Birmingham, U.K. (e-mail: viktor.dremin@bmecenter.ru).

Color versions of one or more figures in this article are available at https://doi.org/10.1109/JSTQE.2025.3533950.

Digital Object Identifier 10.1109/JSTQE.2025.3533950

I. Introduction

Recently, the laser speckle contrast imaging (LSCI) method has been extensively used to visualize microcirculation processes in biological tissues in various medical and scientific aspects [1], [2], including visualization of cerebral blood flow [3], [4], [5], [6]. In particular, LSCI was used to assess cerebral perfusion in experiments in rats [7], [8], [9], [10], [11], mice [12], [13], piglets [14], [15], [16] and even cats [17]. However, one of the most widely used model organisms to study the physiology and pathology of the cerebral circulation is still a laboratory rat.

Despite the fact that LSCI allows to estimate perfusion on a relatively large area of the brain, thus reducing the spatial variability of the recorded parameters, the issue of the influence of the skull bones (and, accordingly, extracerebral blood circulation) on the quality and informative value of the assessment of cerebral perfusion itself (in pial vessels) remains essential. Biological tissues are spatially highly heterogeneous and consist of dynamic inclusions (blood, lymph) and static (skin, bones, etc.) components. This scattering system does not satisfy the ergodicity condition, which can lead to a systematic error of the LSCI method and, as a result, to an incorrect interpretation of the data obtained [18]. Static components can elevate speckle contrast values and artificially inflate the calculated perfusion [19], [20].

In this regard, in addition to developing new algorithms for calculating perfusion and improving measurement methods, an appropriate selection of cranial preparations is required when high-resolution studies are performed on the brain of a laboratory animal. In vivo skull preparations can vary in terms of the size of the skull window and the type of skull modifications. The choice of preparation depends on the type of research method being used, the region of interest and the length of the experiments being planned. Therefore, today there are several forms of cranial preparation being used in research: open cranial window [21], [22], closed cranial window [23], [24], cranial window with access port [25], thinned skull [21], [26], transparent skull [27], [28], polymer skull [29], [30] and some others.

Previous LSCI experiments indicate that in 1-month-old rats, blood microvessels could be visualized quite clearly using through-skull (transcranial) imaging [8], and that method has also been well-proved in mice experiments [4], [31], [32]. In contrast, for mature rats (4 months and older), a cranial preparation

is surely needed in order to map the blood microvessels, as the probing depth of the LSCI method is less than the bone thickness of adult animals. However, it is debatable whether there should be some sort of cranial preparation for young animals (aged 1.5-3 months) or not. In terms of preventing damage to dura mater, all types of cranial windows are excluded from the acceptable methods, as the complete removal of skull bone is very likely to be traumatic for animals of that age. On the contrary, skull bone thinning appears to be a promising and acceptable method, as it preserves the dura mater and does not require special polymer inserts or optical clearing agents.

While studying cerebral blood flow, it is helpful to perform various physiological tests. In particular, the assessment of central hemodynamic parameters during blood loss is crucial in clinical practice. In hemorrhagic and other types of shock, disturbances in microcirculation, perfusion and oxygenation are key pathogenetic factors in the development of organ dysfunction. The sensitivity of LSCI to detect abnormalities in cerebral circulation in the case of a distinct decrease in systemic and cerebral perfusion pressure is understudied. This determines the relevance of preliminary investigations conducted on laboratory animals when modelling hemorrhagic shock.

Thus, the aim of this study was to identify the need for skull thinning in the assessment of cerebral perfusion by the LSCI method in young 1.5-month-old rats with incomplete cranial osteogenesis. An additional objective of the study was to evaluate the sensitivity of LSCI to detect changes in cerebral microcirculation during hemorrhage.

II. Materials and Methods

A. Experimental Protocol

Experiments were carried out on male Wistar rats (1.5 months) weighing 125–140 g (n = 8). Study design: a prospective randomized controlled experimental study in laboratory animals (*in vivo*). Food was withdrawn from the animals 3 hours before the start of the experiment, while they continued to have free access to water. Animal experiments were carried out according to the European Union guidelines for the care of laboratory animals (Directive 2010/63/EU). The study protocol was approved by the Ethics Committee of Orel State University (Protocol No. 27, dated 17/05/2023).

The animals were anesthetized with a combination of tiletamine/zolazepam (Zoletil 100, Virbac, France) 20 mg/kg + xylazine (Xylanite, NITA-PHARM, Russia) 5 mg/kg intraperitoneally. An additional injection of Zoletil 100 at a dose of 10 mg/kg was done in case of a decrease in the depth of anesthesia (response to a painful stimulus). The animals breathed spontaneously during the experiment. For invasive blood pressure (BP) measurement and arterial blood sampling, the left carotid artery was catheterized with a PE -50 polyethylene catheter (OD 0.95 mm, ID 0.58 mm, SciCat, Russia) according to the previously described method [33]. To maintain patency of the catheter, it was flushed with 0.1–0.2 ml of unfractionated heparin (20 EU/ml). After catheterization of the carotid artery, the rat was restrained in a prone position on the heated platform of the Rodent Surgical Monitor+ (INDUS Instruments, USA) with the animal's head fixed in a holding device at three points (upper incisors and ear holders). A rectal thermometer was attached to measure the core body temperature. To maintain the target core temperature (36.0–36.5 °C), animals were warmed using a heated platform. Additionally, to monitor the animal's condition, an ECG was taken by means of electrodes built into the platform.

To expose the parietal bones, a midline incision was made in the skin and soft tissues of the rat's head. The edges of the wound were spread apart in the lateral direction and surgical hemostasis was performed if necessary. The surface of both parietal bones was cleaned with gauze wipes and moistened with warm saline. Measurements of physiological variables at baseline were performed after 15-20 minutes of stabilization of the animal.

To measure blood pressure, the Deltran DPT-100 pressure transducer (Utah Medical Products, USA) was connected to an installed arterial catheter via an infusion line. The analog pressure signal was transmitted from the transducer to the BP-100 device (CWE, Inc., USA) and displayed on its digital screen in the form of systolic, diastolic and mean arterial pressure (MAP) values. MAP values were registered over a 5-minute measurement period.

To obtain LSCI perfusion data, a specially developed experimental setup was assembled. A high-speed UI-3360CP-NIR-GL CMOS camera (IDS, Germany) was used to acquire raw monochrome images with a frame rate of equal to 90 frames per second and exposure time of equal to 11 ms for all conducted experiments. To reduce specular reflection from the measured object, a NIR linear polarizer (Thorlabs, USA) was placed in front of the MVL25TM23 camera objective (Thorlabs, USA). The illumination of the area of interest was performed using the LDM785 laser source (Thorlabs, USA) with a light power of 20 mW and a wavelength of 785 nm. As the chosen light source has a collimated laser beam, the illumination was delivered through the set of diffusers (Thorlabs, USA). An overview of the setup is shown in Fig. 1.

The experiment consisted of 3 stages. At each stage there were two regions of interest (ROIs) as shown in Fig. 2(a). After measuring blood pressure and transcranial LSCI perfusion at baseline (stage 1), all animals underwent skull thinning. The left parietal bone in the projection of the rat sensorimotor cortex was thinned using a dental drill and a set of cutters. The dura mater remained intact, which was confirmed by postmortem examination of the intervention area and measurement of the thickness of the bone plate (∼0.3 mm).

The coordinates of the center of the thinned area were 3 mm caudal to the Bregma line and 2.5 mm lateral to the median suture. The dimensions of the thinned area was about 3× 3 mm. During skull thinning, the bone surface was regularly moistened with saline to avoid overheating and excessive tissue damage. Moisturizing the bone surface was also performed before each LSCI perfusion recording. 5 minutes after skull thinning, MAP and LSCI perfusion were measured again (stage 2). In addition, arterial blood samples (0.2ml) were taken in a heparinized syringe for gas and acid-base state (ABS) testing (pH, pCO_2, pO_2, BE, HCO_3^-, SaO_2, lactate). It was performed using CG4+ cartridges for the iSTAT 1 analyzer (Abbott Point of Care Inc., USA). Such analysis allows to confirm that animals' ABS parameters are within normal limits, and the blood flow recorded

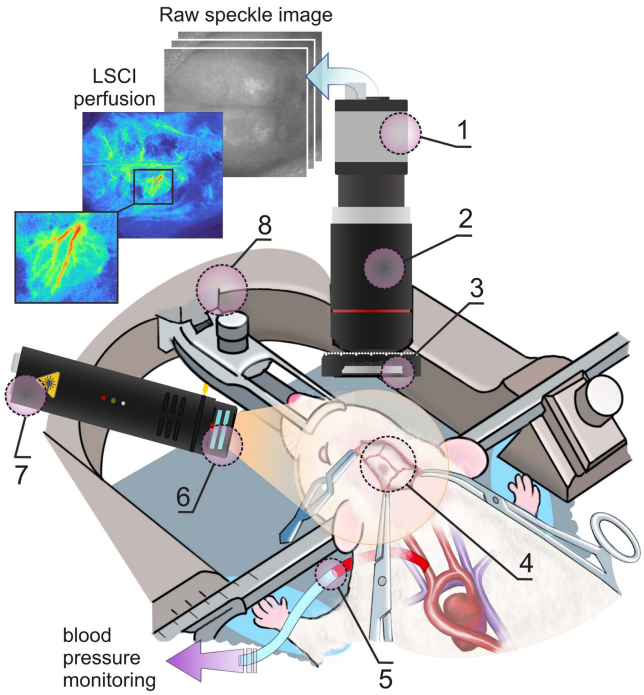

Fig. 1. Scheme of the developed LSCI experimental setup and auxiliary equipment (illustration by K.N. Lapin): 1 – NIR CMOS camera; 2 – camera lens; 3 – NIR linear polarizer; 4 – investigated area; 5 – catheter in carotid artery; 6 – diffusers DG120 and DG1500; 7 – 785 nm laser source; 8 – stereotaxis.

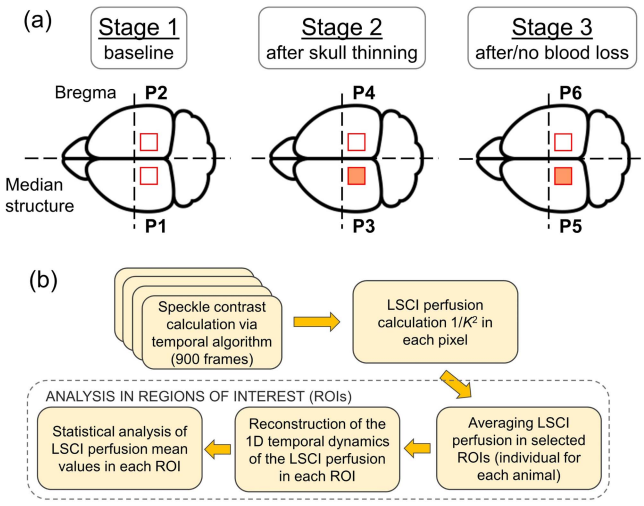

Fig. 2. (a) Stages of the experiment and a scheme of ROIs' positions (filled areas are skull thinning areas). (b) Flowchart of LSCI data processing explaining the steps of the analysis algorithm of the selected ROIs.

during the experiment will depend on physiological stimulus and not on the initial disorders in animals' condition.

Furthermore, to assess the effect of blood loss on cranial and cerebral blood flow, the animals were divided into two groups: a false intervention group (sham, n=4) and a hemorrhage group (hemorrhage, n=4). In a hemorrhage group, a fixed-volume hemorrhage model was used [34]. The estimated blood volume (EBV) in a rat was taken to be 6.5% of body weight. The target blood loss was 30% of the EBV. Blood was drawn from the arterial catheter into a syringe within 5 minutes (10% of the EBV at the 1st, 3 rd and 5th minutes). If the patency of the catheter is impaired during blood sampling, it was washed with a small amount (0.1–0.2 ml) of unfractionated heparin 5 U/ml, after which blood sampling was resumed. The studied physiological variables were recorded again 5 minutes after the end of blood loss (stage 3).

For a false intervention group, there were no procedures after skull thinning, which means that the animal rested for approximately 15 minutes with the following recording of required parameters (stage 3).

At the end of each experiment, the animal was sacrificed by intraarterial injection of lidocaine solution (2%) under general anesthesia with asystole detection in ECG.

B. LSCI Data Processing

The sequence of steps taken to process the data is shown in Fig. 2(b) and specified below. The raw speckle images were processed using an original algorithm developed in the Matlab R2019b software. It allows processing of spatial, temporal, or spatio-temporal speckle contrasts depending on the aim of the processing. Accordingly, using the temporal or spatial standard deviation of the speckle intensity, the average speckle contrast can be calculated as follows:

$$K = \frac{\sigma}{\langle I \rangle}, \tag{1}$$

where $\langle I \rangle$ is the mean intensity value and σ is the intensity standard deviation.

If moving scattering particles are present in the object illuminated by coherent light, then the blurring of the speckle image recorded by the camera will result in the observed standard deviation of the intensity being lower than for a completely static set of scatterers, and therefore the speckle image contrast will also be reduced. Thus, during processing it is possible to obtain speckle-contrast images which reflect high blood flow intensity in the form of a low speckle-contrast value. As mentioned above, this approach does not take into account the influence of static components, but it is widely used in various studies and implemented in most commercial systems. That is why we decided to focus on the study of the behavior of this parameter.

Alongside laser speckle contrast images, it is worth noting that there is also a possibility to obtain laser speckle perfusion images. That is achieved by recalculating laser speckle contrast values into laser speckle perfusion values as $1/K^2$. Such method described in studies on the equivalence and differences between LDF and laser speckle contrast analysis and is proven to present LSCI data in the form that is similar to LDF perfusion [35], [36], [37], [38].

To better visualize the brain vessels, we processed raw speckle images with a number of frames for a temporal average of 900. Thus, the data were averaged over 10 seconds of recording. For further quantitative analysis, the analysis steps remained the same. The spatial algorithm was not applied in these studies to maintain a high quality of visualization and to avoid excessive non-uniformity of data. Hence, 30 samples were obtained during the 5 minutes of recording analyzed for each ROI in each animal.

TABLE I
THICKNESS OF BONE PLATE IN RATS; IN THIS TABLE AND FURTHER: (S) STANDS FOR SHAM ANIMAL AND (H) STANDS FOR HEMORRHAGE ANIMAL

Rat	1 (H)	2 (H)	3 (S)	4 (H)	5 (S)	6 (H)	7 (S)	8 (S)
Thickness without skull thinning, mm	0.70	0.75	0.65	0.65	0.60	0.70	0.60	0.70
Thickness in thinned area, mm	0.43	0.30	0.30	<0.30	<0.30	<0.30	<0.30	0.30

To quantify the visual data, a calculation of the mean speckle-perfusion values was performed. Two regions of interest in the right and left hemispheres of the rat brain were selected for analysis. In ROI in the right hemisphere, the skull bones were intact throughout all stages of the experiment, whereas in ROI in the left hemisphere, thinning of the skull bone occurred before the stage 2 of the experiment. The placement of ROIs was mirrored in relation to the median suture. The ROI's size was constant throughout three stages of the experiment for each animal and equaled the size of a thinned area for both ROIs (in the left and right hemispheres). However, it should be noted that ROI's size slightly varied from one animal to another as the thinning area for each rat turned out to be different in dimensions.

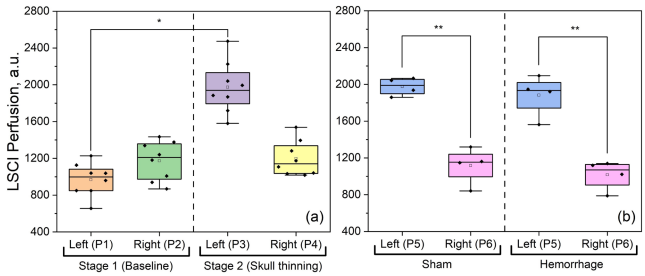

Fig. 3. (a) LSCI perfusion values in the left and right hemispheres of the rat brain before and after left-sided skull thinning and (b) LSCI perfusion values in the left (thinned) and right (intact) cerebral hemisphere in rats with and without hemorrhage. * Statistically significant differences for $p < 0.05$ in the Wilcoxon Signed Ranks Test; ** Statistically significant differences for $p < 0.05$ in the Mann–Whitney U Test.

C. Statistical Analysis

The sample size was not calculated due to the lack of literature data on the variability of the studied LSCI variables in rats. To test the statistical significance of differences in the obtained data, the following criteria were applied: Mann-Whitney U Test and Wilcoxon Signed Ranks Test. The Mann-Whitney U test was used to compare LSCI perfusion indices in the left and right sides of the skull (within the framework of the stage of the experiment). The Wilcoxon Signed Ranks Test was used to assess changes in variables over time (in different stages of the experiment).

III. RESULTS

To confirm that the dura mater remained intact after skull thinning, a post-mortem measurement of the thickness of the bone plate was performed. The acquired results are shown in Table I. It validates that skull thinning was performed correctly and there were no bone punctures, which means that the thinning process had not damaged cerebral blood vessels.

When analyzing the data for each rat, an average perfusion value of 5 minutes was obtained for each stage of the study in each ROI, so that each point in the following graphs represents a value for one of the rats. The values for all 8 rats for the baseline and skull thinning stages are presented in Fig. 3(a). At the baseline (stage 1), LSCI perfusion did not differ between the left (P1) and right (P2) ROIs of the rat skull ($p > 0.05$ in the Mann-Whitney U test). The MAP at the baseline for all rats was 78.0 [73.5; 88.7] mmHg. After thinning of the left parietal bone (stage 2), LSCI perfusion on the left side (P3) was higher both compared to the opposite right side (P4, $p < 0.05$ in the Mann-Whitney U test) and compared to previous values in the same ROI (P1, $p < 0.05$ in the Wilcoxon Signed Rank test). The MAP in the animals at this stage of the experiment was 77.0 [73.9; 83.0] mmHg.

As mentioned above, in stage 3, the animals were divided into two groups. In both groups (hemorrhage and sham), the values of LSCI perfusion on the left (thinned) side of the skull remained higher compared to the intact right side (P5 vs P6, $p < 0.05$ in the Mann-Whitney U test). At the same time, the studied groups of animals did not differ in the values of LSCI perfusion measured in P5 and P6 ROIs while compared in the groups and pair-wise between the groups Fig. 3(b), despite the fact that the MAP at stage 3in the hemorrhage group was lower than in the sham group (50.5 [46.9; 54.8] vs 69.0 [60.4; 69.6], correspondingly). All obtained MAP values are shown in Table II.

Arterial blood gases were assessed and acid-base analysis was performed in all animals at stage 2 after measuring MAP and cerebral perfusion, results are presented in Table III. The pH and pCO_2 values were within the reference range for rats [39], [40]. However, in some animals, pO_2, SaO_2, BE and bicarbonate levels were reduced during anesthesia and surgery (moderate oxygenation impairment and compensated metabolic acidosis).

Next, each group of animals (sham and hemorrhage) was considered individually. The results for sham group are shown in Fig. 4(a). For perfusion values in the thinned area and in the intact area, statistically significant differences ($p < 0.05$ in Mann–Whitney U Test) among the left and right hemisphreres were revealed at the stage 2 of the experiment (P3 vs P4), and also at the stage 3 (P5 vs P6). In contrast to the previous group, hemorrhage animals demonstrated more uneven results amongst themselves, however, there were still a statistically significant differences ($p < 0.05$ in Mann-Whitney U Test) between the left and the right area at stages 2 (P3 vs P4) and 3 (P5 vs P6). The results are shown in Fig. 4(b).

TABLE II
MAP FOR ALL STAGES OF THE EXPERIMENT

Rat	1 (H)	2 (H)	3 (S)	4 (H)	5 (S)	6 (H)	7 (S)	8 (S)
MAP1, mmHg	73.5	129.0	93.0	87.3	75.0	81.0	73.5	70.0
MAP2, mmHg	104.5	77.0	89.0	77.0	70.5	72.0	81.0	74.5
MAP3, mmHg	54.0	57.0	36.0*	47.0	69.5	46.5	70.0	68.5

*The animal exhibited an inadequate decrease in MAP at the given stage (a single case).

TABLE III
GASES AND ACID-BASE STATE OF RAT'S ARTERIAL BLOOD AT STAGE 2: PCO_2 – PARTIAL PRESSURE OF CO_2 IN ARTERIAL BLOOD, MMHG; pO_2 – PARTIAL PRESSURE OF O_2 IN ARTERIAL BLOOD, MMHG; BE – BASE EXCESS, HCO_3^- – ANION BICARBONATE, MMOL/L; SaO_2 – ARTERIAL BLOOD OXYGEN SATURATION, %; LAC – LACTATE LEVEL, MMOL/L

Rat	1 (H)	2 (H)	3 (S)	4 (H)	5 (S)	6 (H)	7 (S)	8 (S)
pH	7.39	7.38	7.37	7.36	7.37	7.39	7.4	7.37
pCO_2	36	33.1	37.4	40.8	36.5	34.9	41.4	42.6
pO_2	77	90	66	50	69	59	84	60
BE	-3	-5	-3	-2	-4	-3	1	-1
HCO_3^-	21.6	19.4	21.6	22.9	21.2	21.4	25.9	24.7
SaO_2	95	97	92	84	93	90	96	90
Lac	1.89	1.83	1.35	1.81	1.58	1.12	1.55	1.05

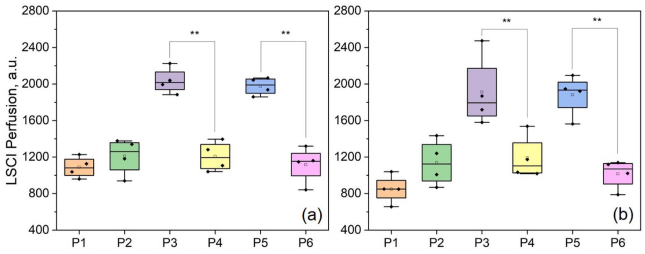

Fig. 4. LSCI perfusion values for (a) sham animals and (b) hemorrhage animals for all stages of the experiment. ** Statistically significant differences for $p < 0.05$ in the Mann-Whitney U Test.

Examples of visualization are shown in Fig. 5. It shows results for a sham-operated animal and for an animal with blood loss. Although the effects of blood loss are not clearly apparent, the need for skull thinning is evident upon examination of these images. LSCI allows us to reveal the vascular architectonics of the studied area as well as to assess the overall blood supply.

IV. DISCUSSION

In regards to this study, the collected data prove the conclusion made earlier based on the visualisation that skull thinning is necessary for proper evaluation of cerebral blood flow even in young animals (1.5-3 months old). Microvascular visualisation is clearly improved by skull thinning, as confirmed by microvascular maps for all rats in the second and third stages of the experiment. Additionally, it can be deduced that a longer time of stabilization of the animal after skull thinning (from 20 minutes and more) is necessary, as the graphs show a decrease of data scattering at the stage 3 for both groups of animals. It is important to let the processes in the blood microcirculation system sufficiently stabilize after thinning to acquire more physiologically correct data.

Upon analysing the investigations previously mentioned in introduction that utilize cranial preparations in rats by means of physical impact (craniotomy, thinning) [21], [22], [23], [24], it is noted that researchers obtained results similar to those we have described in this paper (with adjustment for the age of the animals studied). Cited studies substantiate the findings of conducted experiments: a cranial preparation of any kind enhances the quality of obtained data; in adult animals that is the only way to get access to cerebral blood flow assessment.

As for the optical clearing methods which does not involve physical damage to the bone tissues, they also demonstrate great potential. Through changes in tissue optical properties [41], it is possible to examine cerebral blood flow both *in vivo* [42] and ex vivo [43]. For all its advantages, the need for a prolonged waiting period to achieve an optimal optical clearing effect and the requirement of special clearing agents made it difficult to use this method in the presented study.

The outcome of studying the effect of blood loss on cerebral microcirculation has been somewhat confounded. The MAP values shown in Table II indicate that blood loss was performed appropriately, and the hemodynamic characteristics of the animals have changed. However, despite the physiological impact through blood loss that is confirmed with the blood pressure values analysis, the speckle perfusion values in the two groups of animals did not have statistically significant differences among themselves.

Regardless of the mild oxygenation and metabolic disturbances detected in the arterial blood gas analysis in some animals, pH and pCO_2 were within normal limits in all rats. This indicates that the increase in cerebral perfusion in stage 2 compared to stage 1 of the experiment is due to skull thinning, and not to pathological changes in these factors regulating cerebral circulation.

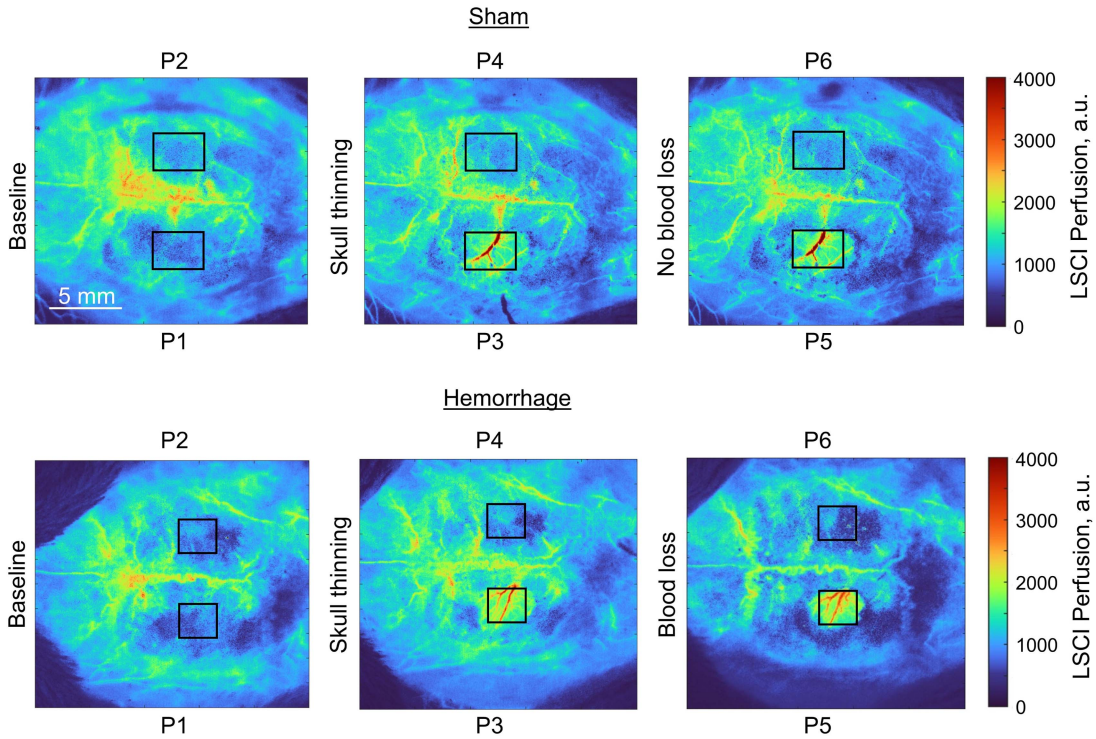

Fig. 5. Examples of laser speckle perfusion images for a rat without blood loss (sham) and for a rat that experienced blood loss (hemorrhage).

In the hemorrhage group, cerebral perfusion in the thinned area did not decrease in stage 3 after blood loss. The most likely explanation for this is that the severity of blood loss (30% of the EBV) was insufficient to reduce MAP below the lower limit of the cerebral autoregulation.

Additionally, microhemocirculatory disorders are known to have specific manifestations depending on the vascular region of the body. These manifestations are determined by the features of the blood supply of a particular organ and the nature of local vascular reactions in response to blood loss. The blood supply of vital organs, such as the brain or heart, can be maintained for some period of time due to the effective autoregulation of blood flow and the centralization of blood circulation [44]. It is important to note that this phenomenon is crucial for the survival of these organs during times of stress or injury.

V. Conclusion

The main finding of our work is confirmation of the need to perform thinning of the skull bones in young 1.5-month-old rats for reliable recording of cerebral perfusion using the LSCI method. It has also been demonstrated that cerebral perfusion in rats does not decrease after moderate blood loss. However, further LSCI studies are needed to assess the impact of alterations in cerebral perfusion due to a disorder of its autoregulation.

Undoubtedly, the LSCI method at the present stage of its development has limitations in both experimental and clinical application. Additionally, our study was limited in the pool of animals. However, the demonstrated results confirm that the assembled LSCI setup is capable of detecting and capturing microcirculation parameters with fine spatial and temporal resolution and may be used to carry out preclinical fundamental studies.

Disclosures

The authors declare no conflicts of interest.

References

[1] E. Zharkikh, V. Dremin, E. Zherebtsov, A. Dunaev, and I. Meglinski, "Biophotonics methods for functional monitoring of complications of diabetes mellitus," *J. Biophotonics*, vol. 13, no. 10, 2020, Art. no. e202000203.

[2] A. Sdobnov, G. Piavchenko, A. Bykov, and I. Meglinski, "Advances in dynamic light scattering imaging of blood flow," *Laser Photon. Rev.*, vol. 18, no. 2, 2024, Art. no. 2300494.

[3] A. K. Dunn, "Laser speckle contrast imaging of cerebral blood flow," *Ann. Biomed. Eng.*, vol. 40, pp. 367–377, 2012.

[4] V. Kalchenko et al., "A robust method for adjustment of laser speckle contrast imaging during transcranial mouse brain visualization," *Photonics*, vol. 6, no. 3, 2019, Art. no. 80.

[5] S. H. Mikkelsen, M. V. Skøtt, E. Gutierrez, and D. D. Postnov, "Laser speckle imaging of the hippocampus," *Biomed. Opt. Exp.*, vol. 15, no. 2, pp. 1268–1277, 2024.

[6] S. S. Kazmi, L. M. Richards, C. J. Schrandt, M. A. Davis, and A. K. Dunn, "Expanding applications, accuracy, and interpretation of laser speckle contrast imaging of cerebral blood flow," *J. Cereb. Blood Flow Metab.*, vol. 35, no. 7, pp. 1076–1084, 2015.

[7] Y. Takeshima et al., "Visualization of regional cerebral blood flow dynamics during cortical venous occlusion using laser speckle contrast imaging in a rat model," *J. Stroke Cerebrovasc. Dis.*, vol. 24, no. 10, pp. 2200–2206, 2015.

[8] N. Golubova, E. Potapova, E. Seryogina, and V. Dremin, "Time–frequency analysis of laser speckle contrast for transcranial assessment of cerebral blood flow," *Biomed. Signal Process. Control.*, vol. 85, 2023, Art. no. 104969.

[9] G. Piavchenko et al., "Impairments of cerebral blood flow microcirculation in rats brought on by cardiac cessation and respiratory arrest," *J. Biophotonics*, vol. 14, no. 12, 2021, Art. no. e202100216.
[10] Y. Shen et al., "Quantification of cerebral vascular autoregulation immediately following resuscitation from cardiac arrest," *Ann. Biomed. Eng.*, vol. 51, no. 8, pp. 1847–1858, 2023.
[11] B. Lee, D. D. Postnov, C. M. Sørensen, and O. Sosnovtseva, "The assessment of cortical hemodynamic responses induced by tubuloglomerular feedback using in vivo imaging," *Physiol. Rep.*, vol. 11, no. 6, 2023, Art. no. e15648.
[12] L. Hricisák et al., "No deficiency compromises inter-and intrahemispheric blood flow adaptation to unilateral carotid artery occlusion," *Int. J. Mol. Sci.*, vol. 25, no. 2, 2024, Art. no. 697.
[13] E. J. Bian, C.-W. Chen, C.-M. Cheng, C.-Y. Kuan, and Y.-Y. Sun, "Impaired post-stroke collateral circulation in sickle cell anemia mice," *Front. Neurol.*, vol. 14, 2023, Art. no. 1215876.
[14] M. L. G. Mikkelsen et al., "The effect of dexmedetomidine on cerebral perfusion and oxygenation in healthy piglets with normal and lowered blood pressure anaesthetized with propofol-remifentanil total intravenous anaesthesia," *Acta Vet. Scand.*, vol. 59, pp. 1–13, 2017.
[15] F. Domoki et al., "Comparison of cerebrocortical microvascular effects of different hypoxic-ischemic insults in piglets: A laser-speckle imaging study," *J. Physiol. Pharmacol.*, vol. 65, no. 4, pp. 551–558, 2014.
[16] F. Domoki et al., "Evaluation of laser-speckle contrast image analysis techniques in the cortical microcirculation of piglets," *Microvasc. Res.*, vol. 83, no. 3, pp. 311–317, 2012.
[17] D. L. Hollenbeck et al., "Sedation with dexmedetomidine decreases skin perfusion in cats," *Amer. J. Vet. Res.*, vol. 84, no. 12, 2023, Art. no. 84.
[18] A. Sdobnov et al., "Speckle dynamics under ergodicity breaking," *J. Phys. D: Appl. Phys.*, vol. 51, no. 15, 2018, Art. no. 155401.
[19] A. B. Parthasarathy, W. J. Tom, A. Gopal, X. Zhang, and A. K. Dunn, "Robust flow measurement with multi-exposure speckle imaging," *Opt. Exp.*, vol. 16, no. 3, pp. 1975–1989, 2008.
[20] B. Liu, D. Postnov, D. A. Boas, and X. Cheng, "Dynamic light scattering and laser speckle contrast imaging of the brain: Theory of the spatial and temporal statistics of speckle pattern evolution," *Biomed. Opt. Exp.*, vol. 15, no. 2, pp. 579–593, 2024.
[21] M. Isshiki and S. Okabe, "Evaluation of cranial window types for in vivo two-photon imaging of brain microstructures," *Microscopy*, vol. 63, no. 1, pp. 53–63, 2014.
[22] H. Soleimanzad et al., "Multiple speckle exposure imaging for the study of blood flow changes induced by functional activation of barrel cortex and olfactory bulb in mice," *Neurophotonics*, vol. 6, no. 1, pp. 15008–15008, 2019.
[23] A. Holtmaat et al., "Long-term, high-resolution imaging in the mouse neocortex through a chronic cranial window," *Nat. Protoc.*, vol. 4, no. 8, pp. 1128–1144, 2009.
[24] C. Ayata et al., "Laser speckle flowmetry for the study of cerebrovascular physiology in normal and ischemic mouse cortex," *J. Cereb. Blood Flow Metab.*, vol. 24, no. 7, pp. 744–755, 2004.
[25] C. J. Roome and B. Kuhn, "Chronic cranial window with access port for repeated cellular manipulations, drug application, and electrophysiology," *Front. Cell. Neurosci.*, vol. 8, 2014, Art. no. 379.
[26] I. J. Biose, D. Dewar, I. M. Macrae, and C. McCabe, "Impact of stroke co-morbidities on cortical collateral flow following ischaemic stroke," *J. Cereb. Blood Flow Metab.*, vol. 40, no. 5, pp. 978–990, 2020.
[27] A. Steinzeig, D. Molotkov, and E. Castren, "Chronic imaging through "transparent skull" in mice," *PLoS One*, vol. 12, no. 8, 2017, Art. no. e0181788.
[28] Y.-J. Zhao et al., "Skull optical clearing window for in vivo imaging of the mouse cortex at synaptic resolution," *Light Sci. Appl.*, vol. 7, no. 2, pp. 17153–17153, 2018.
[29] C. Heo et al., "A soft, transparent, freely accessible cranial window for chronic imaging and electrophysiology," *Sci. Rep.*, vol. 6, no. 1, 2016, Art. no. 27818.
[30] L. Ghanbari et al., "Cortex-wide neural interfacing via transparent polymer skulls," *Nat. Commun.*, vol. 10, no. 1, pp. 1–13, 2019.
[31] M. Z. Ansari, E.-J. Kang, M. D. Manole, J. P. Dreier, and A. Humeau-Heurtier, "Monitoring microvascular perfusion variations with laser speckle contrast imaging using a view-based temporal template method," *Microvasc. Res.*, vol. 111, pp. 49–59, 2017.
[32] Y. N. Kalyuzhnaya et al., "An alternative photothrombotic model of transient ischemic attack," *Transl. Stroke Res.*, 2024.
[33] K. Lapin, I. Ryzhkov, V. Maltseva, and E. Udut, "Vascular catheterization in small laboratory animals in biomedical research: Technological aspects of the method," *Bull. Sib. Med.*, vol. 20, no. 3, pp. 168–181, 2021.
[34] A. Fülöp, Z. Turóczi, D. Garbaisz, L. Harsányi, and A. Szijártó, "Experimental models of hemorrhagic shock: A review," *Eur. Surg. Res.*, vol. 50, no. 2, pp. 57–70, 2013.
[35] Y. Li et al., "Predicting the ischemic infarct volume at the first minute after occlusion in rodent stroke model by laser speckle imaging of cerebral blood flow," *J. Biomed. Opt.*, vol. 18, no. 7, pp. 076024–076024, 2013.
[36] H. Cheng and T. Q. Duong, "Simplified laser-speckle-imaging analysis method and its application to retinal blood flow imaging," *Opt. Lett.*, vol. 32, no. 15, pp. 2188–2190, 2007.
[37] I. Mizeva et al., "Wavelet analysis of the temporal dynamics of the laser speckle contrast in human skin," *IEEE Trans. Biomed. Eng.*, vol. 67, no. 7, pp. 1882–1889, Jul. 2020.
[38] I. Mizeva, E. Potapova, V. Dremin, I. Kozlov, and A. Dunaev, "Spatial heterogeneity of cutaneous blood flow respiratory-related oscillations quantified via laser speckle contrast imaging," *PLoS One*, vol. 16, no. 5, 2021, Art. no. e0252296.
[39] M. Brun-Pascaud, C. Gaudebout, M. Blayo, and J. Pocidalo, "Arterial blood gases and acid-base status in awake rats," *Respir. Physiol.*, vol. 48, no. 1, pp. 45–57, 1982.
[40] R. K. Subramanian et al., "Normative data for arterial blood gas and electrolytes in anesthetized rats," *Indian J. Pharmacol.*, vol. 45, no. 1, pp. 103–104, 2013.
[41] A. N. Bashkatov et al., "Measurement of tissue optical properties in the context of tissue optical clearing," *J. Biomed. Opt.*, vol. 23, no. 9, pp. 091416–091416, 2018.
[42] D. Zhu, K. V. Larin, Q. Luo, and V. V. Tuchin, "Recent progress in tissue optical clearing," *Laser Photon. Rev.*, vol. 7, no. 5, pp. 732–757, 2013.
[43] A. Jaafar, M. E. Darvin, V. V. Tuchin, and M. Veres, "Confocal raman micro-spectroscopy for discrimination of glycerol diffusivity in ex vivo porcine Dura Mater," *Life*, vol. 12, no. 10, 2022, Art. no. 1534.
[44] R. Schlichtig and M. R. Pinsky, "Defining the hypoxic threshold," *Crit. Care Med.*, vol. 19, no. 2, pp. 147–149, 1991.

Nadezhda Golubova received the B.Sc. and M.Sc. degrees in 2020 and 2022, respectively, from Orel State University, Orel, Russia, where she is currently working toward the Ph.D. degree with the R&D Center of Biomedical Photonics. Since 2021, she has been a Research Assistant with the R&D Center of Biomedical Photonics, Orel State University. She has been a coauthor in works on applying imaging technologies in cases of studying blood microcirculation, both through laparoscopic equipment and without it. Her research interests include biomedical imaging and optical non-invasive diagnostics of biological tissues and mainly focuses on the application of optical technologies that utilize dynamic light scattering for biotissue diagnostics.

Ivan Ryzhkov received the M.D. degree from the Faculty of Medicine, Sechenov University, Moscow, Russia, in 2009, and the Ph.D. degree in pathophysiology and critical care medicine on the topic "microcirculation disorders in the skin and brain in acute blood loss and their correction" in 2020. In 2011, he completed his Clinical Residency in anesthesiology and intensive care medicine, and he was a Physician with the Department of Anesthesiology and Intensive Care, N.I. Pirogov National Medical and Surgical Center, Moscow, Russia. He began working as a Researcher in the field of pathophysiology of critical illness. Since 2018, he has been the Head with the Laboratory of Experimental Research, Federal Research and Clinical Center of Intensive Care Medicine and Rehabilitology, Russian Federation. He has authored and coauthored more than 20 articles in refereed journals, three patents, and two book chapters. His research interests include cardiac arrest and resuscitation, cardiovascular pathophysiology, microcirculatory disorders in hemorrhagic shock, laser methods for studying microcirculation (LDF, LSCI), and laboratory animal anesthesia.

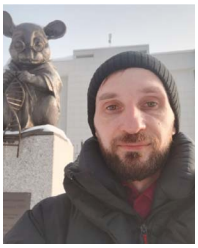

Konstantin Lapin received the Graduation degree from the Faculty of Biology, Moscow State Academy of Veterinary Medicine and Biotechnology named after K. I. Scriabin, Moscow, Russia, in 2005. During his studies, he actively participated in various scientific events of the Academy, for which he was the recipient of the Diplomas and Commendations. He conducted scientific work in Katun and Karadag Nature Reserves. He was a Researcher with the Lopukhin Federal Research and Clinical Center of Physical-Chemical Medicine and the Institute of Cell Biophysics of the Russian Academy of Sciences. He is currently with Federal Research and Clinical Center of Intensive Care Medicine and Rehabilitology. He is also the Founder and Head of the Scientific Company SciCat, which manufactures catheters for laboratory animals.

Evgeniya Seryogina received the M.Sc. degree in biomedical engineering in 2020 from Orel State University, Orel, Russia, where she is currently working toward the Ph.D. degree in biology. Since 2015, she has been participating in the research within the Research and Development Center of Biomedical Photonics and is also a Member with Orel State University SPIE Student Chapter. Started in 2018, she is Researcher with Cellular Physiology and Pathology Laboratory, Research and Development Center of Biomedical Photonics. She has authored and co-authored more than 30 articles in refereed journals and conference proceedings and one patent. Her H-index 8, i10-index six (Google Scholar, 04.2024). Her research interests include biomedical imaging, optical tools for assessment of metabolic activity of biological tissues and cells, in vivo modeling on cell cultures and laboratory animals. She was the recipient of various prestigious National and International awards.

Andrey Dunaev received the M.Sc. and Ph.D. degrees from Orel State University, Orel, Russia, in 1999 and 2002, respectively. He is currently a Leading Researcher with the R&D Center of Biomedical Photonics, Orel State University. He is also an Honorary Worker of Science and High Technologies with Russian Federation. Under the supervision of Prof. Dunaev, six doctoral theses were successfully defended. He is an author and co-author of more than 200 papers in peer-reviewed journals and conference proceedings, eight monographs and more than 15 patents. His H-index is 26, i10-index is 62 (Google Scholar, 04.2024). His research interests include multimodal optical diagnostics of microcirculatory-tissue systems, focusing on methodological and metrological support of diagnostic systems. He is also a Senior Member of SPIE.

Viktor Dremin received the M.Sc. and Ph.D. degrees from Orel State University, Orel, Russia, in 2013 and 2017, respectively. During the first several years of his career, he was involved in the development of new scientific devices for optical remote sensing of the Earth and Terrestrial Planets as an Optoelectronics Design Engineer with Astron Electronics, Russia. As a Ph.D. degree Student, he conducted active research in biomedical engineering and biophotonics with the R&D Center of Biomedical Photonics, Orel State University, Russia. Part of his Ph.D. degree research was carried out with Aston University, Birmingham, U.K., by Erasmus+ Programme. After Ph.D. degree viva in 2017, his work on the development of an imaging system for skin chromophores visualisation has been supported by EDUFI Fellowship, Finland. He has authored and coauthored more than 100 articles in refereed journals and conference proceedings, 11 patents, and four book chapters. His H-index 27, i10-index 54 (Google Scholar, 11.2024). His research interests include biomedical imaging, optical tools for assessment of metabolic activity of biological tissues, and modelling of optical radiation propagation in biological tissues. In 2019, his project to develop a multimodal hyperspectral system for the diagnosis of glycation of biological tissues was the recipient of the support of a prestigious Postdoctoral Grant by Marie Skłodowska-Curie Individual Fellowships Programme, and the various prestigious National and International awards.

Elena Potapova received the Medical Assistant degree from Orel Base Medical College, in 2003, and the M.Sc. and Ph.D. degrees from Orel State University, Orel, Russia, in 2004 and 2008, respectively. Since 2018, she has been a Senior Researcher with the R&D Center of Biomedical Photonics, Orel State University. She has been a co-author on works on integrating spectroscopy and imaging technologies with standard surgical equipment to enable optical diagnostics during fine needle biopsy and laparoscopic procedures for various pathologies. Her H-index 14, i10-index 23 (Google Scholar, 04.2024). Her research interests include biomedical imaging and different biophysical experiments in area of optical non-invasive diagnostics, and mainly focuses on the development of technology for multiparametric optical biopsy in minimally invasive surgical procedures.